International Journal of Advanced Research and Review

www.ijarr.in

STRUCTURAL, ELECTRONIC AND OPTICAL PROPERTIES OF WURTZITE AND ZINC BLENDE InN WITH GGA AND mBJ POTENTIAL

Lalrintluanga Sailo[1*], Ricky L. Ralte[2], Z. Pachuau[3], C. Lalramliana[4]

[1]Research Scholar, Department of Physics, Mizoram University, Aizawl, India
[2]Assistant Professor, Department of Electronics, Govt. Zirtiri Residential Science College, Aizawl, India
[3]Professor, Department of Physics, Mizoram University, Aizawl, India
[4]Assistant Professor, Department of Mathematics, Govt. Serchhip College, Serchhip, India
***Corresponding Author:** Department of Physics, Mizoram University, Aizawl, India. Pin: 796004. Email:lalrinasailo@gmail.com

ABSTRACT

To obtainthe parameters of InN semiconductor compound in wurtzite (WZ) and zincblende (ZB) structures, we have carried out a first-principle total-energy calculation of the structural, electronic and optical properties for WZ and ZB InN semiconductor with density functional theory with Generalized Gradient Approximations (GGA) and modified Becke–Johnson (mBJ) potential. To find the best parameters for each structure, we have optimized the total energy as a function of the unit cell volume and the c/a ratio for the wurtzite structure and for zincblende structure, the total energy as a function of the unit cell volume and the lattice parameter. Our calculations have shown agreement with the other theoretical and experimental results. The electronic band structures were calculated from the optimized lattice parameter with GGA and mBJ potential using Full Potential Linearized Augmented Plane Wave (FP-LAPW) method. The optical properties, including the real and imaginary part of dielectric function, reflectivity, refractive index, absorption coefficient, electron energy loss function and optical conductivity of WZ and ZB InN semiconductor under ambient conditions are discussed.

Keywords: DFT; FP-LAPW; structure optimization; optical properties; mBJ-GGA.

1. INTRODUCTION

Group III-nitrides AlN, GaN, InN and their alloys which had been studied extensively in the last decades, are becoming one of the most important semiconducting materials. GaN and their alloys with In are used in a variety of commercial optoelectronic devices, including green and blue light emitting diodes (LEDs) and even highly efficient white light LEDs [Nakamuraet al. (2000), Steranka et al. (2002)]. Group III-nitrides have also found applications in other electronic devices and all these advancements were due to the advances in its synthesis. Though AlN and GaN have been studied extensively and its properties are also quite well established, studies were few in InN owing to the difficulties in the preparation of good quality single crystals, leaving many of the key parameters of this material difficult to determine. For this reason, InN has been the least studied of the group III-nitrides. The low concentration, high mobility samples synthesized by Foley and Tansley (1986) showed a strong absorption edge at 1.9 eV that corresponds to the fundamental energy gap of InN. This bandgap near 2 eV was confirmed by other groups, using sputtering

techniques for the film growth [Westraet al. (1988), Kubota et al. (1989)]. Davydov et al.(2001) reported the observation of both a strong absorption onset and bright photoluminescence (PL) located below 1 eV for InN films grown by MBE. This was followed by other reports from Wu et al.(2002) and Matsuoka et al.(2002) who confirmed that MBE and MOCVD-grown InN was showing a bandgap near 0.7 eV. The prospect of a bandgap near 0.7 eV generated much interest as it raised the possibility that the nitrides could be used to make optical devices which operated from the UV to the infrared (IR), which is of great interest for optoelectronic applications. Many other MBE and MOCVD groups confirmed the presence of the 0.7 eV feature as debate continued over the merits of PL and absorption in determining the bandgap in the InN case. The availability of high-quality single crystals has created the opportunity for the systematic investigation of the fundamental properties of InN. The optical absorption, photoluminescence (PL), and photo modulated reflection (PR) measured on MBE-grown InN with low electron concentrations have shown that the energy gap of InN is 0.67 ± 0.05 eV, almost one-third of the previously accepted value[Davydovet al. (2001), Wu et al. (2002), Nanishi et al. (2003)]. The low energy gap has found support in band structure calculations [Bechstedt et al. (2003), Carrier and Wei (2005)].

2. COMPUTATIONAL METHOD

2.1. THEORY AND METHOD USED

The total energy calculations are performed using WIEN2k package based on FP-LAPW method[Blaha et al. (2014)]. The exchange correlation effect is treated using Perdew - Burke - Ernzerhof - Generalized Gradient Approximation (PBE-GGA) [Perdew et al. (1996)] and modified Becke-Johnson -Generalized Gradient Approximation (mBJ-GGA) [Becke and Johnson (2006),Tran and Blaha (2009)]. In this method, the unit cell is split into non-overlapping muffin-tin spheres of radius (RMT) around the atomic sites and an interstitial region. Different basis sets are used for these regions. The equilibrium volume V_0, bulk modulus B_0, pressure and derivative of bulk modulus B_0' are determined by fitting the total energy versus the reduced and extended volume of the unit cell into third-order Birch-Murnaghan's equation of state [Schulz, and Thiemann(1977),Wyckoff (1986)] as:

$$E(V) = E_0 + \frac{9V_0B_0}{16}\left\{\left[\left(\frac{V_0}{V}\right)^{2/3} - 1\right]^3 B_0' + \left[\left(\frac{V_0}{V}\right)^{2/3} - 1\right]^2 . \left[6 - 4\left(\frac{V_0}{V}\right)^{2/3}\right]\right\} \quad (1)$$

$$P(V) = \frac{3B_0}{2}\left[\left(\frac{V_0}{V}\right)^{7/3} - \left(\frac{V_0}{V}\right)^{5/3}\right] . \left[1 + \frac{3}{4}\left(B_0' - 4\right)\left\{\left(\frac{V_0}{V}\right)^{2/3} - 1\right\}\right] \quad (2)$$

where E_0 is the total energy; V_0 is the equilibrium volume; B_0 is the bulk modulus at pressure P=0.

2.2. STRUCTURAL PROPERTIES

In wurtzite InN structure, InN has 4 atoms in its unit cell, two In atoms and two N atoms. The space group is $P6_3mc$. The atomic positions of In are (2/3, 1/3, 0) and (1/3, 2/3, 1/2). The atomic positions of N are (2/3, 1/3, *u*) and (1/3, 2/3, 1/2+*u*), where *u* is the dimensionless internal parameter that represents the relative displacement between the In plane and its nearest-neighbor N plane along the *c* direction. The plane wave cutoff was set to $RMT \times K_{max}$= 7, where *RMT* is the smallest atomic muffin-tin sphere radius and K_{max} is the maximum value of the wave vector in the plane wave expansion. Non-spherical contributions to the charge density and potential within the MT spheres were considered up to l_{max}= 10, while the charge density. The *MT* spheres radii (*RMT*) used were 2.0 a.u. for In while it was 1.7 a.u. for N. In the computation, we differentiate between the core-shell electrons of In ($1s^2$

$2s^2\ 2p^6\ 3s^2\ 3p^6\ 3d^{10}\ 4s^2\ 4p^6\ 4d^{10}$) & N ($1s^2$); and the valence electrons of In ($5s^2\ 5p^1$) and N ($2s^2\ 2p^3$). The self-consistent potentials were calculated on a dense mesh of 10,000 k-points in the first Brillouin zone (BZ), and the convergence criterion was set to 10^{-4} Ry. We have used experimental lattice parameters for InN: a = 3.533Å and c = 5.693Å as a starting point for optimization. Geometry minimization and optimization of internal parameters were done using the code 2Doptimize and –mini program in the WIEN2k code. The volume optimization curve is shown in Fig 1. Our calculations for structural properties by using Murnaghan equation of state are summarized in Table-1 along with other computational and experimental results for comparison.

2.3. OPTICAL PROPERTIES

The optical properties of solids provide an important tool for studying energy band structure, impurity levels, excitons, localized defects, lattice vibrations, and certain magnetic excitations. The optical response of a material to the electromagnetic field at all energy levels can be described by means of complex dielectric function ε(ω), which is directly related to the energy band structure of solids.

$$\varepsilon(\omega) = \varepsilon_1(\omega) + i\varepsilon_2(\omega) \tag{3}$$

where $\varepsilon_1(\omega)$ and $\varepsilon_2(\omega)$ are real and imaginary part of the dielectric function. There are two contributions to complex dielectric function ε(ω), namely intraband and interband transitions. The contribution from intraband transitions is influential only for metals. The interband transitions can be further divided into direct and indirect transitions [Kong and Jiang (2009)]. Here the indirect interband transitions are neglected, which includes ascattering of phonon and are expected to give only little contributions to ε(ω) [Smith (1971)].The imaginary part $\varepsilon_2(\omega)$ of dielectric function is [Okoye (2003)]:

$$\varepsilon_2(\omega) = \frac{4\pi^2 e^2}{\Omega^2 m^2 \omega^2} \int d\vec{k} \left| \vec{e}.\vec{M}_{cv} \right|^2 \delta\left(E_c - E_v - \hbar\omega\right) \tag{4}$$

Real part $\varepsilon_1(\omega)$ of the dielectric function can be found from its corresponding $\varepsilon_2(\omega)$ by Kramers-Kronig transformation[Jackson (2007)]:

$$\varepsilon_1(\omega) = 1 + \frac{2}{\pi} P \int_0^{\infty} \frac{\omega'}{(\omega')^2 - \omega^2} \varepsilon_2(\omega') d\omega' \tag{5}$$

where *P* denotes the principal part of the integral. From the knowledge of $\varepsilon_1(\omega)$ and $\varepsilon_2(\omega)$, all the other optical properties can be calculated [Jackson (2007)].

$$R(\omega) = \frac{(n-1)^2 + \kappa^2}{(n+1)^2 + \kappa^2} \tag{6}$$

$$n(\omega) = \frac{\sqrt{\varepsilon_1^2(\omega) + \varepsilon_2^2(\omega)} + \sqrt{\varepsilon_1(\omega)}}{\sqrt{2}} \tag{7}$$

$$\kappa(\omega) = \frac{\sqrt{\varepsilon_1^2(\omega) + \varepsilon_2^2(\omega)} - \sqrt{\varepsilon_1(\omega)}}{\sqrt{2}} \tag{8}$$

$$L(\omega) = \frac{\varepsilon_2(\omega)}{\varepsilon_1^2(\omega) + \varepsilon_2^2(\omega)} \tag{9}$$

where *n* is the real part of the complex refractive index (refractive index) and κ is the imaginary part of the refractive index, called extinction coefficient and also reflectivity R(ω), energy loss function L(ω).

3. RESULTS AND DISCUSSION

3.1. STRUCTURAL PROPERTIES

The ground state equilibrium lattice parameters (a_0 and c_0), anion position parameter u, equilibrium volume (V_0), bulk modulus (B_0) and its pressure derivative (B_0') calculated, for both wurtzite and zincblende InN are shown in Table-1. The present values are in good agreement with the experimental values and other reported theoretical values [, , ,] which are in reasonable agreement with our calculation.

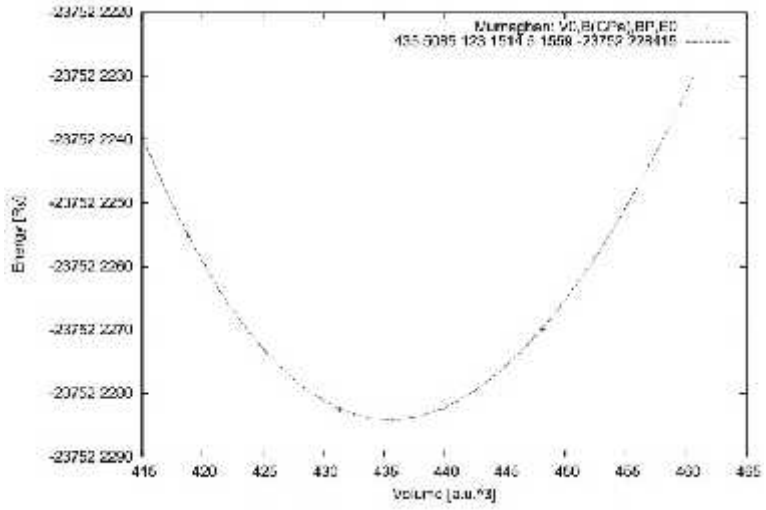

(a)

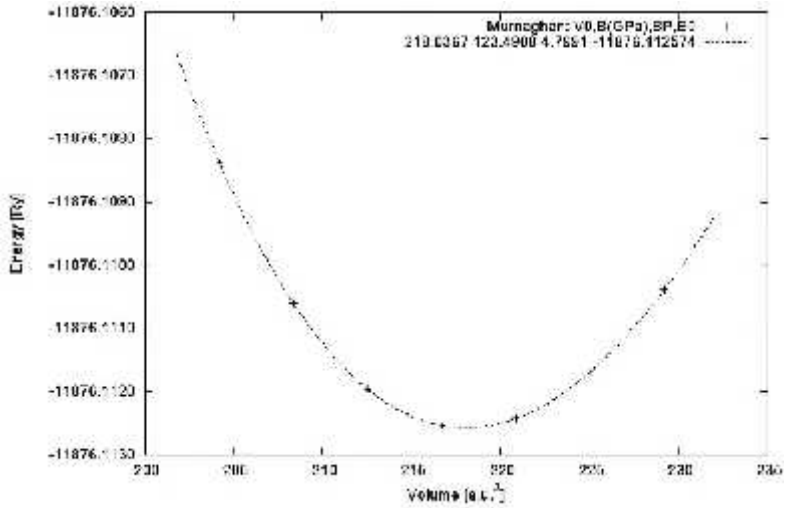

(b)

Fig1. Calculated value of Total Energy versus Total Volume for (a) WZ-InN (b) ZB-InN.

Table-1. Calculated structural parameters with experimental data and other calculations.

	WZ InN		ZB InN	
	Our calculation	**Other results**	**Our calculation**	**Other results**
a (Å)	3.6248	3.587 [a] 3.533 [b]	5.0559	4.949 [d] 4.98 [e]
c/a	1.557	1.614 [a] 1.611 [b]	-	-
u	0.378	0.376[a]	-	-
V (a.u.)^3	435.508	406.62 [c]	218.0367	-
B (GPa)	123.1514	146.31 [c]	123.49	142.9[d] 137 [e]
B_0	5.1559	4.5989[c]	4.7991	4.672 [d]

[a]Carvalhoet al. (2011), [b]Alsardiaet al. (2015), [c]Benkabouet al. (1993), [d]Strite (1993),[e]Carrier and Wei (2005).

3.2. ELECTRONIC PROPERTIES

The electronic structures of InN were calculated with the optimized lattice constant using GGA and mBJ potential as shown in Fig 2 and 3. The Fermi energy is set at 0 eV. In all calculations, the top of the valence band maxima (VBM) and the conduction band minima (CBM) occur at Γ point, showing that InN in both structures is a direct band gap between VBM and CBM.

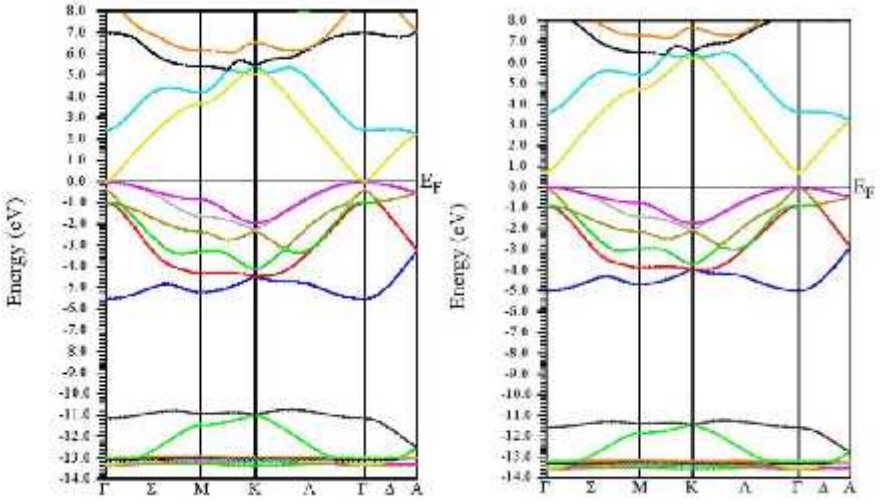

(a) **(b)**

Fig 2. Band structures using (a) GGA (b) mBJ for WZ InN.

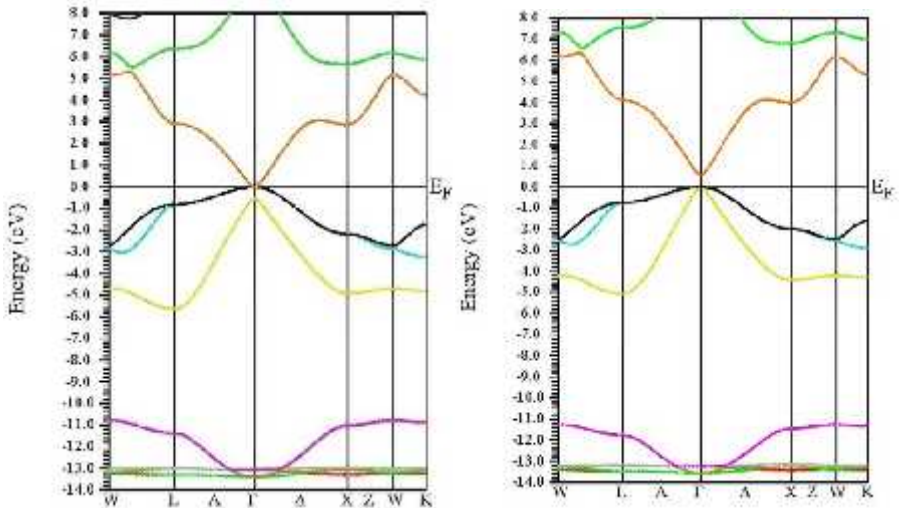

(a) **(b)**

Fig 3. Band structures using (a) GGA (b) mBJ for ZB InN

The GGA calculation underestimated the band gap in both WZ and ZB structure, as compared to the experimental values as shown in Table 2. The implementation of new mBJ potential resolved this discrepancy of band gap from GGA results and provided an almost exact value as compared to experimental and other theoretical results. The CBM has been shifted towards the higher energy than that of the GGA results but the position of VBM is shifted least, almost fixed at the calculated GGA position. The calculated band gap are -0.02 and 0.73 eV for WZ InN with GGA and mBJ respectively while a value of - 0.02 and 0.56 eV is obtained for ZB InN with GGA and mBJ potential.

Table-2. Calculated band gaps of InN, compared with other experimental and theoretical results.

Compounds	Methods/XC	Eg (eV)
WZ-InN		
This work	GGA	-0.02
	mBJ	0.73
Experiment	-	0.780[a]
Other calculations	LDA+C[a]	0.85
	mBJ-LDA[b]	1.162
ZB-InN		
This work	GGA	-0.02
	mBJ	0.56
Experiment	-	0.700[a]
Other calculations	LDA	-0.480[c]
	GGA-EV	0.141[d]

[a]Carrier and Wei (2005), [b]Wei et al. (2003), [c]Ahmeda et al. (2005), [d]Ahuja (1996).

3.3. OPTICAL PROPERTIES

As seen from the band structure calculation, mBJ calculation gives better result compared to GGA calculation and hence, mBJ potential is used for all further calculations. The detailed variation of real, $\varepsilon_1(\omega)$ and imaginary $\varepsilon_2(\omega)$ parts of the dielectric function for wurtzite and zinc blende InN with photon energy are shown in Figs. 4(a) and (b).

As wurtzite crystal has hexagonal symmetry, we need to calculate two different independent principle components for $\varepsilon(\omega)$ such as $\varepsilon(\omega)_{zz}$ and $\varepsilon(\omega)_{xx}$ corresponding to light

polarized parallel and perpendicular to c-axis. Due to this reason, all optical constants are compared together in two directions. The $\varepsilon_1(\omega)$ spectra appear at the same energy as a peak in the corresponding $\varepsilon_2(\omega)$ spectra.

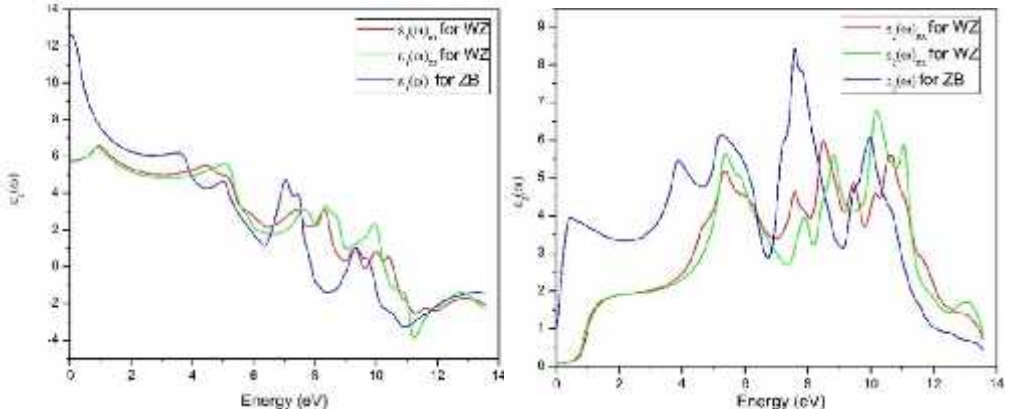

(a) **(b)**

Fig 4. (a) Real part of dielectric function $\varepsilon_1(\omega)$ and (b) Imaginary part of dielectric function $\varepsilon_2(\omega)$ as a function of photon energy for WZ and ZB InN.

Our analysis of the $\varepsilon_2(\omega)$ curves show that the first critical points of the dielectric function occur at 0.72 eV, and 0.7 eV for wurtzite and zinc blende InN respectively. These critical points are followed by a small structure located at 1.73 eV in wurtzite and 2.3 eV in zinc blende InN related to direct transition (L - L). The main peaks in the spectra are situated at 8.34 eV and 7.82 eV respectively for wurtzite and zinc blende InN. The main peak is followed by pronounced peak situated at 10.94 eV and 10.26 eV. These peaks are primarily due to direct transition between the valence band and conduction band above the Fermi energy at L-edge. We observed considerable anisotropy in the imaginary and real part of the dielectric function of wurtzite InN in the range 3.5-13.5 eV, while they are isotropic in the lower energy region. This anisotropy in the optical properties is expected for low symmetry crystals.

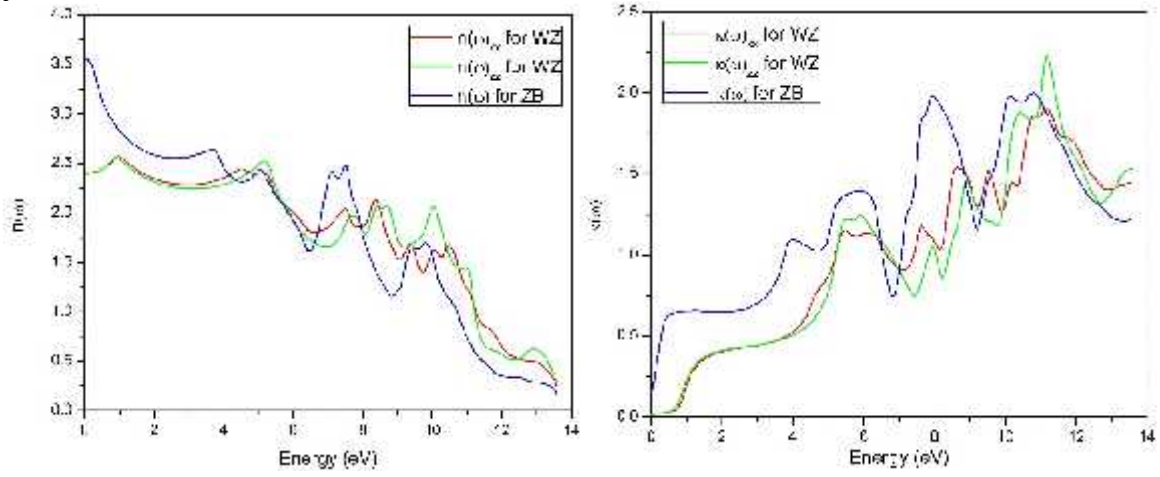

(a) **(b)**

Fig 5. (a) Calculated refractive index n(ω) and (b) extinction coefficient κ(ω) of WZ and ZB InN.

Fig 5.(a) and (b) show the refractive index and extinction coefficient of WZ and ZB InN. Refractive index of an optical medium is a dimensionless quantity that describes the propagation of beam through that medium while the extinction coefficient κ(ω) indicates the strongest absorption at the edge and above 11.2 and 8 eV for WZ and ZB InN respectively,

which lie in the UV region. We calculated the birefringence Δn(0) is equal to 0.006 for wurtzite InN.

The calculated real and imaginary parts of optical conductivity as a function of photon energy are shown in Fig 6.(a) and (b). The real part of the optical conductivity $\sigma_1(\omega)$ is related to the frequency dependent dielectric function $\varepsilon_2(\omega)$ in all frequencies. The peaks in $\sigma_1(\omega)$ are mainly from the interband transitions between the occupied and unoccupied states.

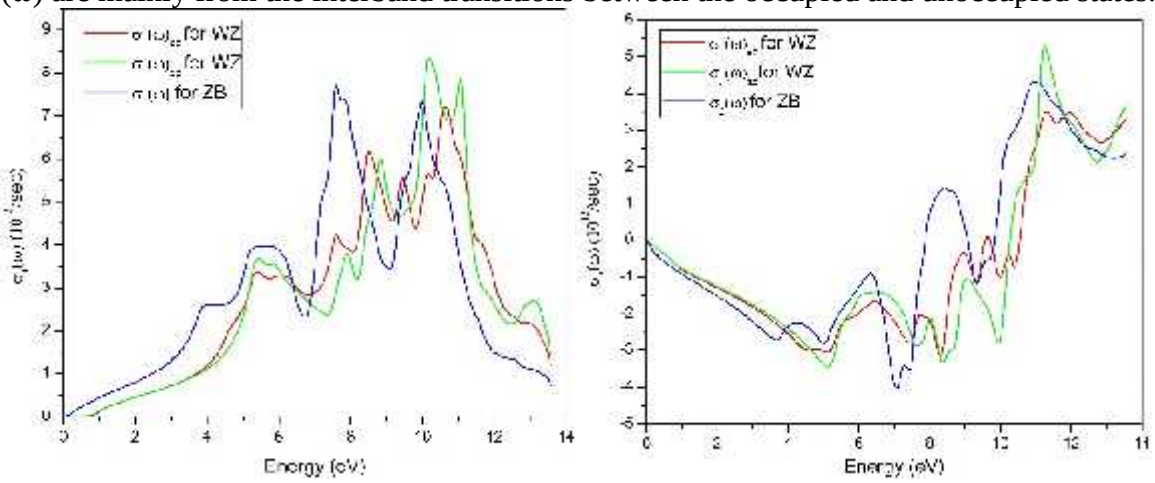

(a) **(b)**

Fig 6. (a) Real and (b) imaginary part of optical conductivity of WZ and ZB InN.

Figs 7.(a) and (b) show the reflectivity and the energy loss spectra for wurtzite and zinc blende InN. The reflectivity is significantly enhanced after 13 eV and 13.5 eV for wurtzite and zinc blende InN respectively. From the figure, we observed that the anisotropy behaviour of wurtzite InN is very small up to 5 eV. The peaks in L(ω) spectra in Fig 7.(b) represent the characteristic combined with the plasma resonance and the corresponding frequency is called plasma frequency (ω_{pl}). The frequency above the plasma frequency shows the dielectric behaviour [$\varepsilon_1(\omega) > 0$] of the material, while its value lower than the plasma exhibits the metallic property [$\varepsilon_1(\omega) < 0$].

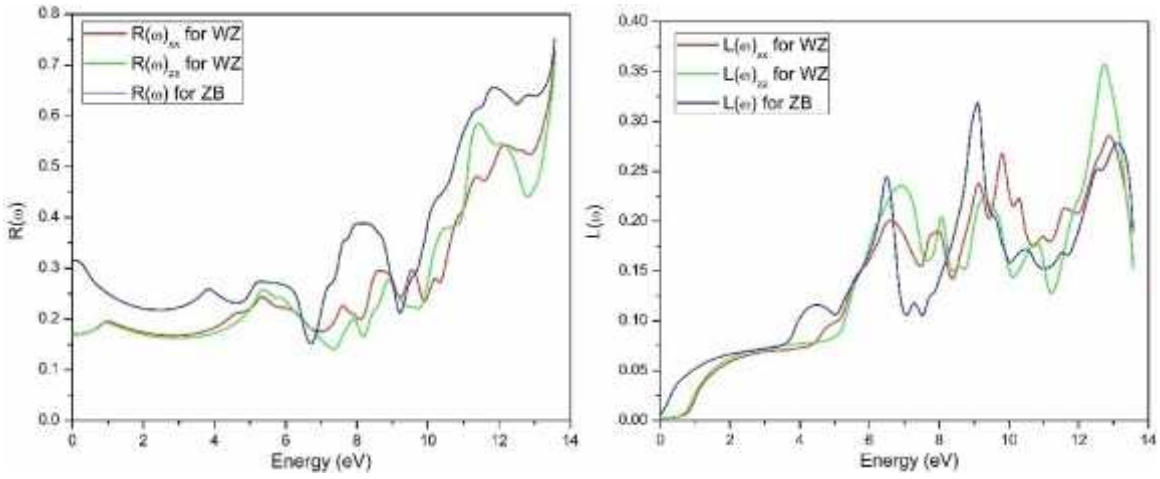

(a) **(b)**

Fig 7. (a) Reflectivity R(ω) and (b) energy loss function L(ω) of WZ and ZB InN.

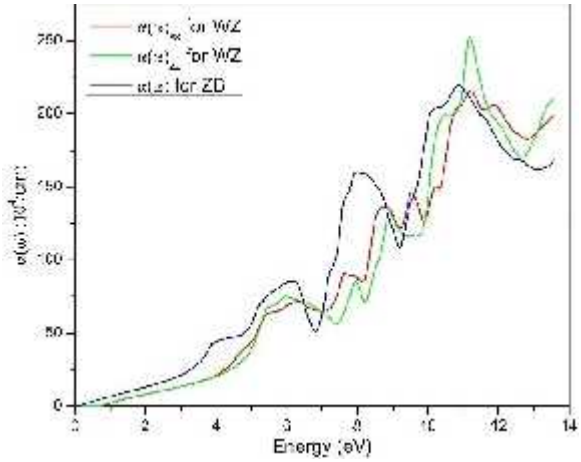

Fig 8. Absorption coefficient α (ω) of WZ and ZB InN.

The calculated absorption coefficient as a function of photon energy is shown in Fig 8.The peaks and valleys represent the possible transition between states in the energy bands.

4. CONCLUSION

In summary, we have calculated the structural, electronic and optical properties of wurtzite and zinc blende InN using Full Potential Linearized Augmented Plane Wave (FP-LAPW) method. Exchange and correlation effects are treated by PBE-GGA and mBJ-GGA potentials. We have verified through calculations that the GGA-ground-state properties of these materials including equilibrium lattice constants, bulk moduli and their first derivatives are consistent with the experimental data and other theoretical calculations. Our calculation provides new structural parameters for the wurtzite and zinc blende InN compounds. The electronic band structure calculations are done using both the exchange correlation potentials. The optical properties, such as real and imaginary parts of dielectric function, reflectivity R(ω), refractive index *n*(ω), extinction coefficientκ(ω), absorption coefficient α(ω), electron energy loss function L(ω) and optical conductivity σ(ω) are calculated within the improved modified Becke-Johnson potential.

REFERENCES

Ahmeda, R., Akbarzadehb, H.and Aleem, F. (2005) A first principle study of band structure of III-nitride compounds", Physica B, 370, 52–60.

Ahuja, R., Eriksson, O., Johansson,B., Auluck,S. and Wills,J.M. (1996) Electronic and Optical Properties of Red HgI_2, Phys. Rev. B, 54, 10419-10424.

Alsardia, M.M., Saeed, M.A., Mahmood, T., Islam, S. and Isa, A.R.M. (2015) DFT Investigations of the Structural and Electronic Properties of XN (Al, Ga, In) Compounds, J. of Adv. in Alloys and Compd., 2(1): 30-36.

Bechstedt, F., Furthmuller,J., Ferhat, M., Teles,L.K., Scolfaro, L.M.R., Leite, J.R., Davydov, V.Y., Ambacher, O.and Goldhahn, R. (2003) Energy gap and optical properties of $In_xGa_{1-x}N$, Phys. Status Solidi a, 195, 628–633.

Becke, A. D. and Johnson, E. R. (2006) A simple effective potential for exchange, J. Chem. Phys., 124, 221101-221105.

Benkabou,F., Certier, M. and Aourang, H. (2003) Elastic properties of Zinc blende GaN, AlN and InN from Molecular Dynamics, Molecular Simulation, 29(3),201-209.

Blaha, P., Schwarz, K., Madsen, G., Kvasnicka, D. and Luitz, J. (2014) An Augmented Plane Wave Plus Local Orbitals Program for Calculating Crystal Properties, Vienna University of Technology, Austria.

Carrier, P. and Wei S.H. (2005) Theoretical study of the band-gap anomaly of InN, J. of App. Phys., 97: 033707.

Carrier, P. and Wei,S.H. (2005) Theoretical study of the band-gap anomaly of InN, J. Appl. Phys., 97(3), p. 033707.

Carvalho, L.C., Schleife, A. and Bechstedt, F. (2011) Influence of exchange and correlation on structural and electronic properties of AlN, GaN, and InN polytypes, Phys. Rev. B, 84: 195105.

Davydov, V.Y., Klochikhin, A.A., Seisyan, R.P., Emtsev, V.V., Ivanov, S.V., Bechstedt, F., Furthmüller, J., Harima, H., Mudryi, A.V., Aderhold, J. and Semchinova, O. (2002) Absorption and emission of hexagonal InN, Evidence of narrow fundamental band gap, Phys. Status Solidi (b), 229(3), r1-r3.

Jackson,J. D. (2007) Classical Electrodynamics, 3rd Edition, Wiley, New Delhi.

Kong, F. J. and Jiang, G. (2009) Nonlinear Optical Response of Wurtzite ZnO from First Principles, Physica B: Condens. Matter, 404: 2340-2344.

Kubota,K., Kobayashi, Y. and Fujimoto, K. (1989) Preparation and properties of III-V nitride thin films, J. Appl. Phys., 66, 2984.

Matsuoka,T., Okamoto, H., Nakao,M., Harima,H. and Kurimoto,E. (2002)Optical bandgap energy of wurtzite InN, Appl. Phys. Lett., 81, 1246.

Nakamura, S., Pearton S. and Fasol G. (2000) The Blue Laser Diode: The Complete Story, Berlin: Springer.

Nanishi, Y., Saito, Y.and. Yamaguchi, T (2003) RF-Molecular Beam Epitaxy Growth and Properties of InN and Related Alloys, Jpn. J. Appl. Phys., 42,2549.

Okoye, C.M.I. (2003) Theoretical Study of the Electronic Structure, Chemical Bonding and Optical Properties of $KNbO_3$ in the Paraelectric Cubic Phase,J. Phys. Condens. Matter, 15, 5945-5958.

Perdew, J.P., Burke, K. and Ernzerhof, M. (1996) Generalized Gradient Approximation Made Simple, Phys. Rev. Lett., 77: 3865-3868.

Schulz, H. and Thiemann, K. H. (1977) Crystal structure refinement of AlN and GaN, Solid State Commun., 23(11): 815-819.

Smith, N.V. (1971) Photoelectron Energy Spectra and the Band Structure of the Noble Metals, Phys. Rev. B, 3, 1862-1878.

Steranka, F.M., Bhat, J., Collins, D., Cook, L., Craford, M.G., Fletcher, R.and Khare, R. (2002) High Power LEDs – Technology Status and Market Applications, Phys. Status Solidi a, 194(2), 380-388.

Strite, S., Chandrasekhar, D., Smith, D.J., Sariel,J., Chen,H., Teraguchi,N. and Morkoç,H. (1993) Structural properties of InN films grown on GaAs substrates: observation of the zincblende polytye, J. Crystal. Growth, 127, 204-208.

Tansley,T.L.and Foley, C.P. (1986) Optical band gap of indium nitride, J. Appl. Phys., 59(9), 3241-3244.

Tran, F. and Blaha, P. (2009) Accurate band gaps of semiconductors and insulators with a semilocal exchange-correlation potential, Phys. Rev. Lett., 102: 226401.

Wei,S.H. (2003) National Center for Photovoltaics and Solar Program Review Meeting, Denver, Colorado.

Wei, S.H., Nie,X., Batyrev, I.G. and Zhang, S.B. (2003) Breakdown of the band-gap-common-cation rule: The origin of the small band gap of InN, Phys. Rev. B, 67, 165209.

Westra,K.L., Lawson,R.P.W. and Brett, M.J. (1988) The effects of oxygen contamination on the properties of reactively sputtered indium nitride films, J. Vac. Sci. Technol. A, 6, 1730.

Wu, J., Walukiewicz, W., Shan, W., Yu, K.M., Ager, J.W., Haller, E.E., Lu, H. and Schaff, W. J. (2002) Effects of the narrow band gap on the properties of InN, Phys. Rev. B, 66: 201403.

Wyckoff, R. (1986) Crystal Structures, 2nd ed., Krieger, Malabar.